Molecular Characterization of Hexaoctyloxy-Rufigallol in the Solid and Columnar Phases: A Local Field NMR Study

Sergey V. Dvinskikh,[†,‡] Zeev Luz,[§] Herbert Zimmermann,[||] Arnold Maliniak,[†] and Dick Sandström*[,†]

Division of Physical Chemistry, Arrhenius Laboratory, Stockholm University, SE−10691 Stockholm, Sweden, Weizmann Institute of Science, Rehovot 76100, Israel, and Department of Biophysics, Max-Planck-Institut für Medizinische Forschung, Jahnstrasse 29, D-69120 Heidelberg, Germany

Received: November 11, 2002

Separated local field NMR spectroscopy was used to obtain $^1H-^{13}C$ dipolar interactions in the solid and columnar phases of the discotic compound 1,2,3,5,6,7-hexaoctyloxy-rufigallol (RufH8O). The couplings were measured and assigned by a variety of advanced NMR techniques performed under both static and magic-angle spinning conditions. The analysis of the dipolar couplings shows that the three nonequivalent aliphatic chains in RufH8O exhibit vastly different structural and dynamical characteristics. It was also found that one of the α methylene signals exhibits two $^1H-^{13}C$ dipolar splittings at low temperatures in the columnar phase. Similar pairs of doublets have previously been observed in a ^2H NMR study of RufH8O$-^2H_\alpha$ and were there interpreted in terms of dynamic packing fluctuations along the columns. We will present an alternative explanation and show that these two doublets most likely originate from nonequivalent protons (or deuterons) in the α methylene group and not from density modulations.

Introduction

Discotic liquid crystals discovered in 1977[1] are formed by disklike mesogens. The molecules usually consist of a rigid aromatic core with aliphatic chains attached in a symmetric way. In most cases, the discotic mesophases exhibit an architecture where the molecules are stacked into columns which in turn form two-dimensional (2D) arrays with various symmetries. Nuclear magnetic resonance (NMR) spectroscopy has established itself as a powerful method for studies of these systems because it can provide detailed information about molecular geometry, average orientation, and dynamics.

In a recent work[2] (hereafter referred to as paper 1), we reported a ^{13}C NMR study of the solid and columnar phases of 1,2,3,5,6,7-hexaoctyloxy-rufigallol (RufH8O), see Figure 1. The phase diagram of RufH8O has previously been determined using DSC measurements,[3−5] X-ray diffraction,[3,5] and ^2H NMR,[3,4] and the following phase transitions were observed

$$\text{solid V} \xrightarrow{2\ ^\circ\text{C}} \text{solid IV} \xrightarrow{19\ ^\circ\text{C}} \text{phase III} \xrightarrow{31\ ^\circ\text{C}} \text{phase II} \xrightarrow{96\ ^\circ\text{C}} \text{isotropic}$$

where III and II are two hexagonal columnar phases. The results in ref 3 indicate that phase V is a true solid in which the side chains are rigid. The transition to phase IV is accompanied by the onset of restricted chain mobility, in phase III the core starts to reorient slowly about the columnar axis, and in phase II the core reorients fast on the NMR time scale.

Our interest in this compound originates from some intriguing features in the ^2H NMR spectra of RufH8O observed by Spiess and co-workers.[3,4] The ^2H data was interpreted in terms of packing modulations along the columnar axis resulting from the incommensurability of the optimal stacking distance of the aromatic core and the aliphatic side chains.[6]

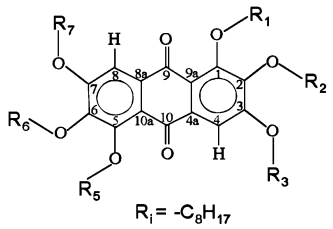

Figure 1. Chemical structure of 1,2,3,5,6,7-hexaoctyloxy-rufigallol (RufH8O) showing the atomic labeling.

In paper 1, we focused on the measurement and assignment of ^{13}C chemical-shift (CS) tensor components in the solid and liquid-crystalline phases of RufH8O using specifically ^{13}C- and ^2H-labeled compounds. Some $^2H-^{13}C$ dipolar couplings were also determined. The ^{13}C CS tensors and $^2H-^{13}C$ dipolar interactions were subsequently used in a conformational analysis of the three nonequivalent side chains in RufH8O. We found that one of the aliphatic chains adopts an in-plane structure, whereas the two other chains prefer out-of-plane conformations.

The strategy in this paper is to extend the investigations of RufH8O by determining $^1H-^{13}C$ dipolar couplings using advanced 2D NMR techniques. The problems of spectral assignment and overlap sometimes encountered in ^2H NMR of complex molecules are to a large extent avoided in these methods because the heteronuclear $^1H-^{13}C$ dipolar interactions are separated by the ^{13}C chemical shifts. Because the dipolar couplings correspond to local magnetic fields, this class of experiments is often referred to as separated local field (SLF) spectroscopy. The dynamical and structural information ex-

* To whom correspondence should be addressed. E-mail: dick.sandstrom@physc.su.se.
[†] Stockholm University.
[‡] On leave from the Institute of Physics, St. Petersburg State University, 198904 St. Petersburg, Russia.
[§] Weizmann Institute of Science.
[||] Max-Planck-Institut für Medizinische Forschung.

10.1021/jp0274381 CCC: $25.00
Published on Web 02/07/2003

tracted from the $^1H-^{13}C$ dipolar couplings is compared with previous results from measurements of ^2H quadrupolar couplings[3,4] and ^{13}C chemical-shift tensors.[2] The NMR measurements were performed at temperatures ranging from -50 to $+85$ °C thus covering all solid and columnar phases. We will also address the issue of density modulations in the columnar phases of RufH8O, and present an alternative explanation of the ^2H spectra reported in refs 3 and 4.

Materials and Methods

Materials. Three different isotopomers of RufH8O were synthesized according to previously described procedures:[7] (i) RufH8O with natural isotopic abundance, (ii) RufH8O specifically labeled with ^{13}C at the α position of the aliphatic chains (RufH8O$-^{13}C_\alpha$), and (iii) α-deuterated RufH8O (RufH8O$-^2H_\alpha$). We also prepared a ^{13}C-diluted sample (RufH8O-10%$-^{13}C_\alpha$) by mixing 10% of RufH8O$-^{13}C_\alpha$ with 90% of the nonlabeled analogue.

Experimental. All NMR experiments were performed at a field of 9.4 T on a Chemagnetics Infinity-400 spectrometer using a 6 mm double-resonance magic-angle spinning (MAS) probe. Ramped cross-polarization[8] (CP) from ^1H to ^{13}C with contact times of 1−3 ms was employed in the solid phases. The CP efficiency is reduced in the mesophase because of molecular reorientation, and we, therefore, sometimes used ^{13}C $\pi/2$ pulses to create transverse magnetization. Sample heating effects due to rotor spinning and/or high-power radio frequency (rf) irradiation were estimated by observing shifts of the phase transition temperatures.

The experiments in the solid phases were performed on powdered (unoriented) samples under MAS conditions. Measurements in the columnar mesophases were carried out on nonspinning samples which were oriented in the magnetic field by slowly cooling from the isotropic phase. This procedure results in a distribution of domains in which all directors are aligned perpendicular to the magnetic field.

2D SLF Experiments. Here we briefly describe the essential features of the NMR techniques employed in this work. For a more thorough discussion, the reader is referred to the original literature cited below.

Two-dimensional SLF spectra in the solid phases were obtained with the pulse sequence shown in Figure 2a. This experiment was recently introduced by Zhao et al.[9] and achieves high spectral resolution in powders because it operates under rapid MAS. During the variable evolution period t_1, the CP-enhanced ^{13}C magnetization evolves in the presence of $R18^7_1$ rf irradiation of the protons. This sequence is based on symmetry arguments in MAS NMR[10−13] and leads to recoupling of $^1H-^{13}C$ dipolar couplings and ^1H chemical-shift interactions, whereas homonuclear dipolar interactions among the ^1H spins are suppressed. The theoretical scaling factor for $R18^7_1$ is equal to 0.182. Proton continuous wave (CW) decoupling is subsequently applied for an interval $T-t_1$ with a ^{13}C π pulse inserted at $^1/_2T$. The duration T is kept constant and equal to an even number of rotor periods. The signal is finally observed during the detection period t_2 as it evolves under the ^{13}C chemical-shift interaction and TPPM ^1H decoupling.[14]

The pulse sequences for the 2D dipolar-shift correlation experiments in the oriented columnar phases are shown in Figure 2b−d. The main difference between the traditional SLF method[15,16] in Figure 2b and the proton-detected local field (PDLF)[17−19] technique in Figure 2c is the way the heteronuclear dipolar interactions are encoded. The PDLF spectra are governed by simple two-spin $^1H-^{13}C$ couplings because the dipolar field is probed

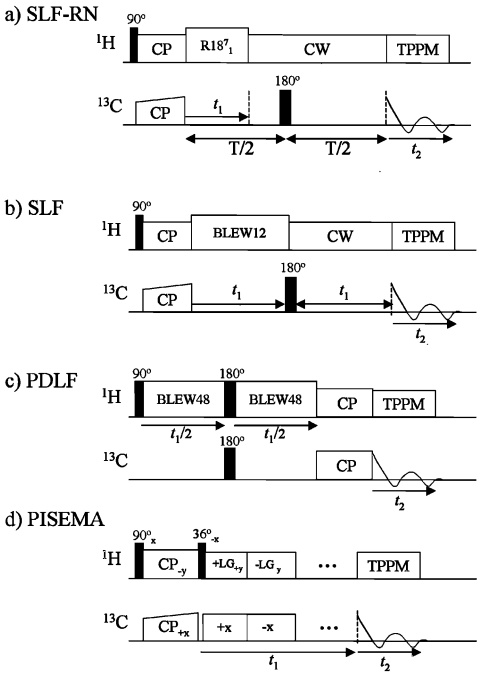

Figure 2. Pulse sequences for 2D local field spectroscopy. All experiments correlate scaled $^1H-^{13}C$ dipolar couplings during t_1 with ^{13}C chemical shifts during t_2. (a) Constant-time sequence for $^1H-^{13}C$ dipolar recoupling under MAS using $R18^7_1$ irradiation. (b) Traditional SLF spectroscopy. (c) PDLF spectroscopy. To increase the spectral width in the dipolar dimension of 2D PDLF spectra, we incremented the evolution period in steps of half of a full BLEW-48 cycle. (d) PISEMA spectroscopy. For all experiments, the TPPM[14] heteronuclear decoupling scheme was used.

at the ^1H spin. This is in contrast to the situation in the SLF experiment in which the ^{13}C magnetization evolves under the simultaneous action of the local magnetic fields from all neighboring protons. The result is a higher multiplicity and a lower sensitivity for the SLF spectra compared to the PDLF spectra. In both SLF and PDLF spectroscopy, it is necessary to remove $^1H-^1H$ homonuclear dipolar couplings during the evolution period t_1, and we have compared the efficiencies of several homonuclear decoupling sequences including MREV-8,[20,21] BLEW-12,[22] and BLEW-48.[22] For RufH8O, it was found that BLEW-12 performed well in the SLF approach, whereas the highest resolution in the PDLF spectra was observed for BLEW-48.

The polarization inversion spin exchange at the magic angle (PISEMA) pulse sequence shown in Figure 2d combines frequency-switched Lee−Goldburg (FSLG) homonuclear decoupling[23−25] with cross-polarization in the t_1 period. The $^1H-^{13}C$ dipolar couplings are monitored through the transient oscillations taking place during the CP process.[26−29]

The multiple-pulse scaling factor for the PDLF sequence was calibrated by observing the scaling of the ^1H frequency offset under BLEW-48 irradiation in a HETCOR-type experiment.[30] The experimental value, 0.420, is in good agreement with the theoretical counterpart 0.424.[22] For the SLF method using BLEW-12 and for PISEMA the theoretical values for the scaling factor, 0.475 and 0.816, respectively, were used.[22,27]

Local field spectroscopy of liquid crystals is often combined with off-magic-angle spinning (OMAS).[19,31] The rapid mechanical sample rotation aligns the director along the spinning axis and leads to scaling of all anisotropic spin interactions. The advantage of OMAS is that lower decoupling fields can be used in order to avoid rf overheating. Preliminary results from local field experiments in the columnar phases of RufH8O indicated

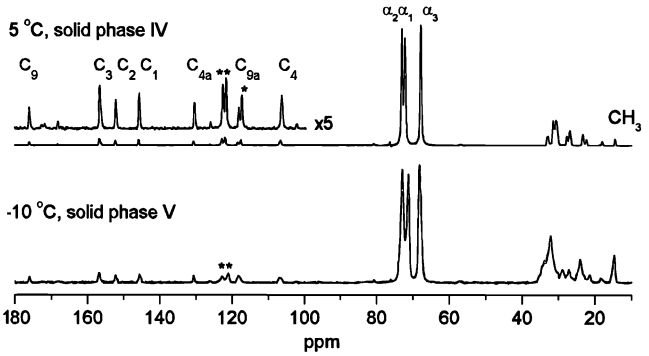

Figure 3. Carbon-13 CP MAS spectra of RufH8O-10%$-^{13}C_\alpha$ in the solid phases IV and V. The asterisks indicate spinning sidebands from the α carbon resonances. The spinning speed and ^1H decoupling field strength were 5 and 70 kHz, respectively. The assignment of C_1 and C_2 is uncertain.

that the heating effect from high-power rf pulses was less than 2 °C for ^1H decoupler field strengths of up to 70 kHz. Because of the high viscosity and flat temperature dependence of the order parameter of our sample, the increase in temperature did not cause any major problems in this study. Therefore, we performed all NMR experiments in the columnar phases under stationary (nonspinning) conditions. The gain is a considerable increase in the resolution of the dipolar peak patterns because the OMAS scaling is avoided.

Numerical Simulations. NMR spectra were simulated using the SIMPSON programming package.[32] Calculations were carried out in the time domain, and the corresponding spectra were obtained by a Fourier transformation. Relaxation effects were taken into account by multiplying the time domain signal with an exponential decay function. The γ-COMPUTE[33] method was used for the simulations of MAS spectra with 9 γ_{CR} angles, and 376 pairs of α_{CR},β_{CR} angles selected according to the scheme of Zaremba,[34] Conroy,[35] and Cheng et al.[36] Parameters describing the molecular geometry were taken from the ab initio calculations presented in paper 1.

Results and Discussion

^{13}C MAS NMR in the Solid Phases of RufH8O. Figure 3 shows the conventional proton-decoupled ^{13}C CP MAS spectra of solid RufH8O-10%$-^{13}C_\alpha$. The peak assignment is taken from paper 1, and the ^{13}C chemical shift of the methyl group is set to 14.5 ppm.[5] The aliphatic signals are quite broad in the low-temperature phase V, which is characteristic of amorphous (disordered) chains. Upon heating to the solid-phase IV, the ^{13}C NMR peaks sharpen and shift slightly showing that the phase transition is accompanied by the onset of restricted chain mobility and/or changes in the molecular structure. It is interesting to note that the number of signals in the aliphatic region of the spectra exceeds the number of chain carbons. In particular, three distinct α methylene signals are observed with an intensity distribution of about 1:1:1. This observation can either be due to nonequivalent molecules in the unit cell or to nonequivalent side chains bonded to the same rufigallol moiety. In paper 1, we showed that the latter explanation was the correct one.

Dipolar cross-sections extracted from a 2D SLF spectrum of RufH8O-10%$-^{13}C_\alpha$ in phase V are shown in Figure 4. These slices are dominated by the $^1H-^{13}C$ dipolar interaction between a ^{13}C spin and its directly bonded proton(s). The effect of weaker couplings to more distant protons is minor.[9]

The only protonated carbon in the aromatic core is C_4 and, as expected, only this ^{13}C site exhibits well-resolved splittings

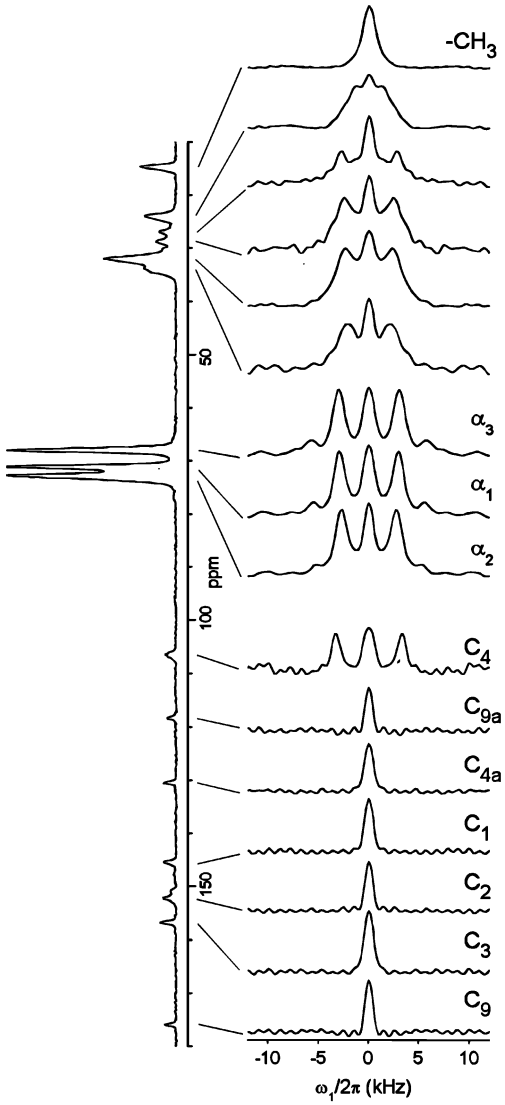

Figure 4. Dipolar cross-sections through a 2D SLF spectrum of RufH8O-10%$-^{13}C_\alpha$ in the solid-phase V at −50 °C. The spectrum was obtained at a spinning speed of 8.0 kHz using the pulse sequence in Figure 2a. The 1D CP MAS spectrum is shown to the left.

in the dipolar dimension. The splitting between the outer two peaks is 6.6 kHz, and the best-fit numerical simulation in Figure 5a shows that this corresponds to a $^1H-^{13}C$ dipolar coupling constant of −23.0 kHz. This value is in agreement with results from aromatic CH groups in rigid systems, and demonstrates the absence of fast core reorientation in the low-temperature phase V.

The α_1 and α_3 methylene subspectra are virtually identical in phase V and correspond to a heteronuclear dipolar coupling of −21.0 kHz (cf. the simulation in Figure 5b). This matches results from rigid CH_2 groups and shows that these two sites are immobile at low temperatures. The dipolar splitting for the α_2 site is reduced by 8% compared to the other two α groups and may be ascribed to small-angle librations. It is worth pointing out that neither the ^{13}C chemical-shift data in paper 1 nor the ^2H spectra[3] of RufH8O were able to provide this very local information on side chain dynamics. The recoupled spectra for the methylene groups located further out in the side chains deviate from the characteristic three-peak feature observed for the α sites. This indicates that the aliphatic chains are not completely frozen in phase V and disagrees with results based on analyses of X-ray diffraction measurements.[3]

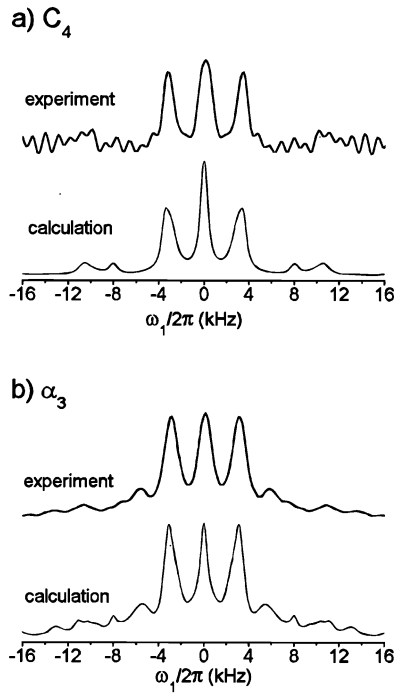

Figure 5. Comparison of experimental and simulated cross-sections for the (a) aromatic carbon C_4 and (b) methylene carbon α_3. The experimental slices are from Figure 4. The simulation in part a used a $^1H-^{13}C$ dipolar coupling constant of -23.0 kHz, a ^1H CSA of -3.8 ppm, and a ^1H asymmetry parameter of 0. The simulation in part b used a $^1H-^{13}C$ dipolar coupling constant of -21.0 kHz, a ^1H CSA of -1.9 ppm, a ^1H asymmetry parameter of 0, and an H−C−H angle of 109.5°.

Representative $^1H-^{13}C$ dipolar slices of RufH8O-10%$-^{13}C_\alpha$, below and above the transition to phase IV, are presented in Figure 6. The splitting of the C_4 subspectrum remains virtually unchanged on going to phase IV, demonstrating that the core is fixed also in the high-temperature solid phase. In contrast, sections through the $^{13}C_\alpha$ peaks change discontinuously when the temperature is raised through the V → IV transition. This suggests the onset of restricted chain dynamics. The motional effect is strongest for the aliphatic chain located between two adjacent chains (α_2) and is only minor for the α_3 signal. Interestingly, chain mobility in phase IV has little effect on the ^{13}C CS tensors of the α carbons (see paper 1). This can be understood if we assume that the only dynamical processes affecting the α methylene sites are librations about the $O-C_\alpha$ bonds. Rapid motions about these chemical bonds strongly modulate the $^1H-^{13}C_\alpha$ dipolar couplings. They do not, however, significantly affect the $^{13}C_\alpha$ CS tensor elements provided that the extreme principal axis direction is close to the $O-C_\alpha$ bond vector and that the asymmetry parameter is small. Such characteristics of the ^{13}C CS tensor have indeed been observed for the α methylene carbons in RufH8O (cf. paper 1). The dipolar splittings for the other aliphatic carbons also decrease in the V to IV transition (not shown).

^{13}C NMR in the Columnar Phases of RufH8O. In the columnar phases, there is a gradual change of the 1D ^{13}C NMR spectra of RufH8O with temperature. No clear indication of the III to II transition is observed. Two examples of ^{13}C spectra of oriented RufH8O-10%$-^{13}C_\alpha$ in mesophase II recorded under static conditions are shown in Figure 7. The peak positions correspond to one of the principal values of the motionally averaged ^{13}C CS tensor. The signals broaden significantly when the temperature is decreased within the mesophase range. We ascribe this behavior to complex interference phenomena between slow molecular reorientation about the columnar axis, ^1H decoupling, and ^{13}C CS interactions.[37,38] It is also worth noting that one of the α signals, α_3, becomes more shielded with respect to the isotropic chemical shift, whereas the other two α peaks move in the opposite direction (cf. Figure 3). The reason for this behavior is that the chemical-shift anisotropies (CSA) for resonances α_3 and α_1/α_2 have different signs, which in turn originate from different conformations of the side chains (see below).

For recording 2D local field spectra in the oriented mesophase, we used the pulse sequences depicted in Figure 2b−d. Among these methods, the PDLF approach provides the highest resolution in our samples. The reason for this is that simple two-spin $^1H-^{13}C$ couplings govern the PDLF spectra because the dipolar field is probed at the abundant spins (^1H) rather than at the rare spins (^{13}C), as in the other experiments.

Figure 8 shows dipolar slices from a 2D PDLF spectrum of RufH8O-10%$-^{13}C_\alpha$ obtained at 85 °C. Each ^{13}C subspectrum consists of a superposition of doublets, with the largest one arising from short-range (often directly bonded) $^1H-^{13}C$ dipolar interactions. The zero-frequency peak originates from unresolved long-range couplings, and its intensity decreases if the CP contact time is shortened (cf. Figure 9a).

The observed splittings in the aromatic region of the spectrum in Figure 8 result mainly from dipolar couplings between core carbons and H_4. Under suitable assumptions, the

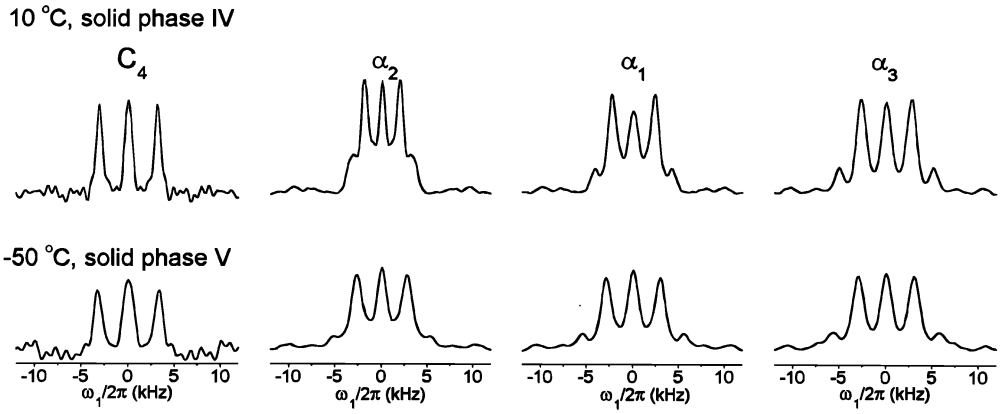

Figure 6. Dipolar cross-sections through 2D SLF spectra of RufH8O-10%$-^{13}C_\alpha$ in the solid phases IV and V. The spectra were obtained at a spinning speed of 8.0 kHz using the pulse sequence in Figure 2a.

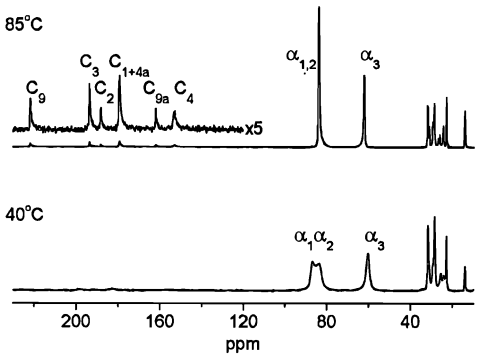

Figure 7. Static ^{13}C spectra of oriented RufH8O-10%$-^{13}C_\alpha$ in the columnar mesophase II.

magnitude of the core $^1H-^{13}C$ dipolar splittings may be written as[39,40]

$$|\Delta\nu| = |\frac{1}{2}kS_{zz}D_{CH}| \quad (1)$$

where

$$D_{CH} = -\frac{\mu_0}{8\pi^2}\frac{\gamma_C\gamma_H\hbar}{r_{CH}^3} \quad (2)$$

is the $^1H-^{13}C$ dipolar coupling constant, k is the multiple-pulse scaling factor, S_{zz} is the orientational order parameter, and r_{CH} is the spin−spin distance. The other symbols have their usual meanings.[16] Using a heteronuclear spin−spin distance of r_{CH} = 1.09 Å, a value of $D_{CH} = -23.3$ kHz is obtained. The directly bonded dipolar splitting in the C_4 cross section is equal to 3.8 kHz, and employing eq 1, we find that the order parameter is 0.78 at 85 °C. In this calculation, a multipulse scaling factor of $k = 0.420$ was used, and contributions from the small isotropic J_{CH} couplings were neglected. The estimated value of the order parameter is typical for columnar phases[41] and agrees with the value obtained using $^2H-^{13}C$ dipolar couplings ($S_{zz} = 0.79$, see paper 1). These order parameters are, however, somewhat lower than the value estimated from the ^{13}C CS tensor analysis ($S_{zz} = 0.85$, see paper 1). The reason for this discrepancy might stem from vibrational effects on the $^1H-^{13}C$ (or $^2H-^{13}C$) bond length.[42]

The experimentally observed splittings due to interactions between C_3-H_4, $C_{4a}-H_4$, and C_9-H_8 are 520, 540, and 300 Hz, respectively (see Figure 8). From the molecular geometry and the order parameter estimated above, the corresponding calculated values are 502, 531, and 295 Hz. For the other core carbons, the splittings are less than 100 Hz and are consequently not resolved in the dipolar slices.

As already discussed, the ^{13}C chemical shifts of the α methylene groups show that the three aliphatic chains are nonequivalent. The analysis of the ^{13}C CS tensors and $^2H-^{13}C$ dipolar couplings in paper 1 indicate that the R_3 side chain prefers an in-plane structure, whereas the others adopt out-of-plane conformations. This structural nonequivalence manifests itself also in the $^1H_\alpha-^{13}C_\alpha$ couplings: the largest dipolar splitting in the α_3 slice is around 2.9 kHz at 85 °C, whereas the splittings for the other two α methylenes are six times smaller (see Figure 8). As we shall see below, these splittings are consistent with the chain conformations discussed above. Although the α_1 and α_2 ^{13}C signals overlap at this temperature, their dipolar splittings are resolved in the indirect dimension (cf. Figure 8). By comparing slices from 2D PDLF spectra of

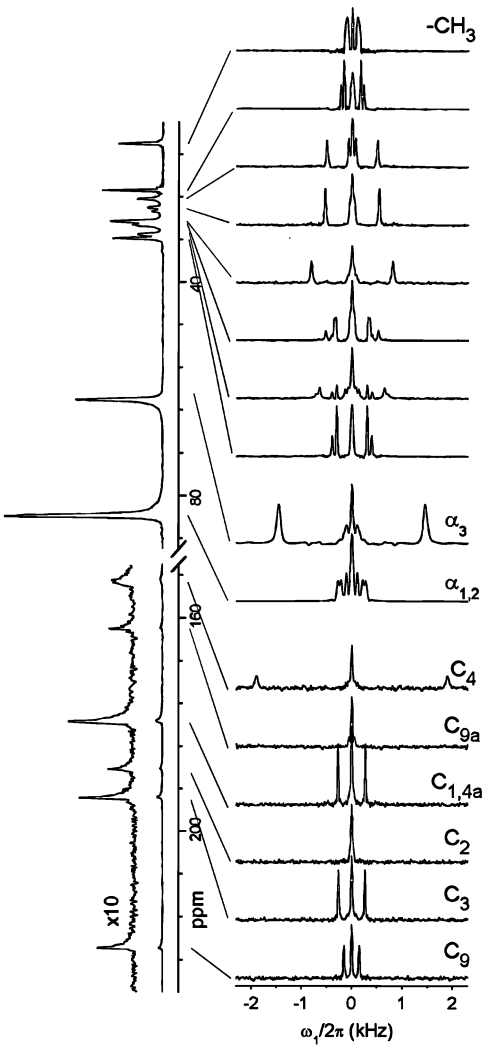

Figure 8. Dipolar cross-sections through a 2D PDLF spectrum of RufH8O-10%$-^{13}C_\alpha$ in the mesophase II at 85 °C. The 1D CP spectrum is shown to the left.

RufH8O-10%$-^{13}C_\alpha$ and RufH8O$-^2H_\alpha$ (see Figure 9), it is clear that the outer two doublets in the $\alpha_{1,2}$ cross-sections in Figure 9a originate from one-bond $^1H-^{13}C$ interactions.

At lower temperatures within the columnar phase, all three α signals are resolved also in the 1D ^{13}C NMR spectrum (cf. Figure 7), which allow for an unambiguous assignment of the $^1H_\alpha-^{13}C_\alpha$ couplings. Cross-sections from a 2D PDLF spectrum of RufH8O-10%$-^{13}C_\alpha$ obtained at 40 °C are shown in Figure 10. It is again obvious that the α methylene groups are nonequivalent in the liquid-crystalline phase. The width of the α_2 subspectrum is smallest. A similar situation prevailed in the solid phases (cf. Figure 6) and indicates that the central chain is more mobile than the other two in both solid and columnar phases.

Another interesting feature in Figure 10 is that the α_3 slice exhibits two dipolar splittings of equal integral intensity. Borrowing ideas from previous investigations of columnar systems,[43] these doublets may be explained by assuming that the α_3 methylene group in RufH8O contains two nonequivalent hydrogen atoms in the low-temperature mesophase. If the two C−H bond vectors have different orientations with respect to the core rotation axis, the resulting $^1H-^{13}C$ local field NMR spectrum will exhibit two doublets.

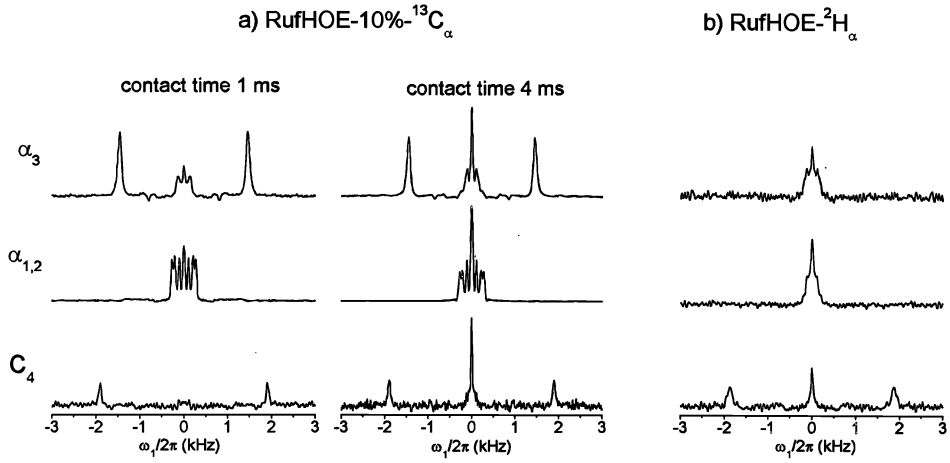

Figure 9. Dipolar cross-sections through 2D PDLF spectra of (a) RufH8O-10%$-^{13}C_\alpha$ and (b) RufH8O-$^{2}H_\alpha$ in the mesophase II at 85 °C.

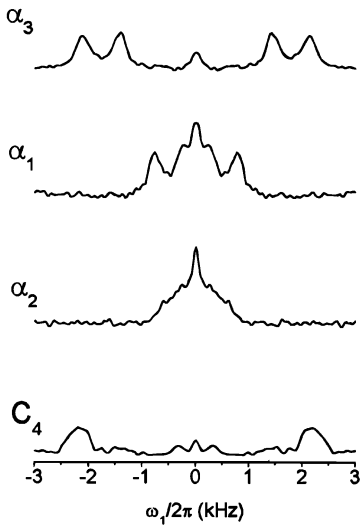

Figure 10. Dipolar cross-sections through a 2D PDLF spectrum of RufH8O-10%$-^{13}C_\alpha$ in the mesophase II at 40 °C.

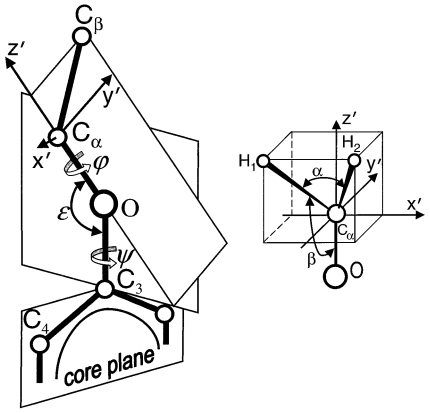

Figure 11. Definition of angles and local frames used in the analysis of the $^{1}H-^{13}C$ dipolar couplings within the α_3 methylene group. The torsion angles φ and ψ are defined by the atoms $C_3-O-C_\alpha-C_\beta$ and $C_4-C_3-O-C_\alpha$, respectively. A definition in which "eclipsed" and "trans" conformations correspond to torsion angles of 0° and 180°, respectively, is used.

To account quantitatively for the observed couplings within the α_3 methylene group, we have analyzed them in terms of side chain structure. By expressing the C−H(1) and C−H(2) bond vectors in a core fixed frame, it is possible to derive the following relationship between the experimental dipolar splittings $\Delta\nu(i)$ and the chain conformation[44]

$$|\Delta\nu(i)| = |\frac{1}{2}kS_{zz}D_{CH}(3\mathbf{V}_{mol}{}^{2}(i)_z - 1)| \qquad i = 1 \text{ or } 2 \quad (3)$$

where $\mathbf{V}_{mol}(i)_z$ is the projection of the C−H(i) bond vector onto the molecular z axis (which coincides with the ring plane normal). This vector is given by

$$\mathbf{V}_{mol}(i) = \mathbf{R}_{y'}(\psi + 90°)\mathbf{R}_{x'}(\epsilon - 90°)\mathbf{R}_{z'}(\varphi)\mathbf{V}(i) \qquad (4)$$

where the matrix $\mathbf{R}_\mu(\gamma)$ ($\mu = x', y', z'$) represents a rotation about the μ axis through an angle γ, and $\mathbf{V}(i) = [\pm\sin(\alpha/2), (\cos^2(\alpha/2) - \cos^2\beta)^{1/2}, -\cos\beta]$ is the unit C−H(i) bond vector expressed in a α methylene fixed frame. The definitions of the angles ψ, φ, ϵ, α, and β are shown in Figure 11. The order parameter S_{zz} at 40 °C was estimated to 0.88 from the C_4 splitting in Figure 10. To solve eqs 3 and 4, contours of ψ and φ which are consistent with the experimental splittings $\Delta\nu = \pm4.2$ kHz (solid lines) and $\Delta\nu = \pm2.9$ kHz (dashed lines) are plotted in Figure 12. The intersections of these lines give the solutions for ψ and φ which simultaneously fit the two dipolar doublets. The analysis of the $^{13}C_\alpha$ CS tensors in the low-temperature mesophase indicates that ψ and ($\varphi - 180°$) for R_3

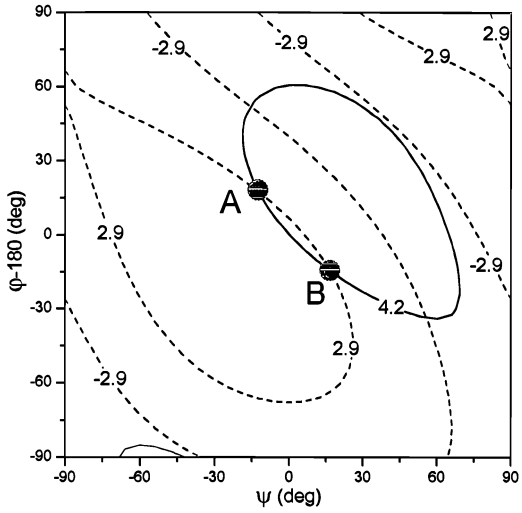

Figure 12. Graphical solution of eqs 3 and 4 for the experimental α_3 dipolar splittings $\Delta\nu = \pm4.2$ (solid lines) and ±2.9 kHz (dashed lines). The intersections of these lines give the possible solutions for the φ and ψ torsion angles. The angles α, β, and ϵ were assumed to be 109°, 109°, and 120°, respectively.

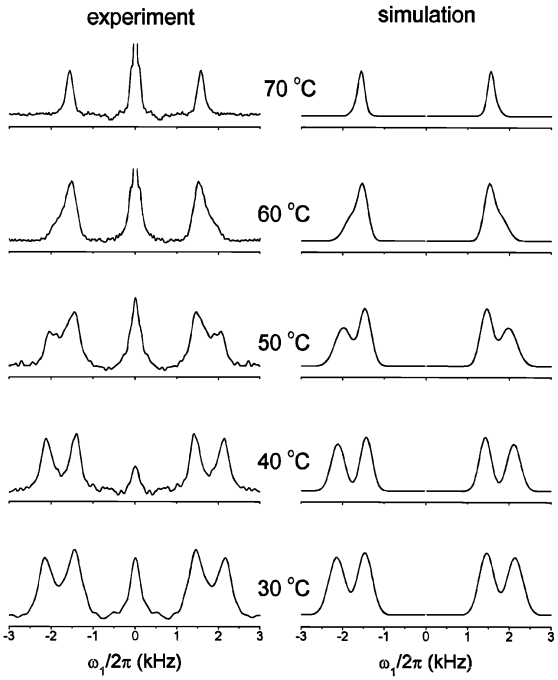

Figure 13. Experimental (left column) and simulated (right column) α_3 cross-sections through 2D PDLF spectra of RufH8O-10%$-^{13}C_\alpha$ versus temperature. Details of the simulations are discussed in the text.

are in the ranges $\pm 20°$ and $\pm 30°$ (see paper 1). Therefore, we deem the solutions labeled A [$\psi = -12°$,($\varphi - 180°$) $= +17°$] and B [$\psi = +17°$,($\varphi - 180°$) $= -14°$] in Figure 12 to be the most probable ones.

In the left column of Figure 13, we show experimental $^1H-^{13}C$ dipolar slices for α_3 as a function of temperature. For each cross-section, an analysis of the type presented above was performed. The torsion angle ψ remains within $\pm 1°$ constant in the entire temperature interval and rules out any large-amplitude motions about the C_3-O bond. This is in agreement with results presented in paper 1. The torsion angle φ exhibits more pronounced temperature dependence. For the solution labeled B in Figure 12, e.g., ($\varphi - 180°$) changes continuously from $-14°$ at 30 °C to $-19°$ at 70 °C. To reproduce the α_3 dipolar subspectra (cf. right column of Figure 13), it was necessary to include a distribution of φ angles. The width of the distribution (assumed to be Gaussian) has a maximum of 6° at 50 °C. However, because we have not considered any local dynamics about the $O-C_\alpha$ bond for α_3, the calculated widths of the φ angle distributions have to be regarded as speculative.

We will now discuss an alternative explanation of the experimental dipolar slices for the α_3 methylene carbon. As shown in Figure 13, these cross-sections exhibit two doublets at low temperatures in the mesophase. By analogy with this observation, a previous ^2H NMR study of RufH8O$-^2H_\alpha$ revealed that one of the aliphatic chains gives rise to two quadrupolar doublets.[3] This was explained by assuming that the two splittings arise from side chains with and without substantial librational dynamics, corresponding to low and high molecular packing densities, respectively. Our interpretation, on the other hand, is based on the assumption that the two doublets originate from nonequivalent protons within the α_3 methylene group. As indicated above, the PDLF method is only sensitive to two-spin $^1H-^{13}C$ interactions and cannot, therefore, distinguish between our explanation and the model based on density modulations. This is analogous to the situation in ^2H NMR spectroscopy since this method produces spectra that are sensitive to only the orientation (and motion) of the $C-^2H$ bond. A more promising approach in this context is to record PISEMA or conventional SLF spectra, which are sensitive to multispin couplings. In the top row of Figure 14, we compare experimental α_3 dipolar slices obtained at 40 °C using the PDLF, SLF, and PISEMA sequences, respectively. Simulations based on two different models are also included. In model I, it is assumed that the spin system consists of a single, isolated methylene ($^1H(1)-^{13}C-^1H(2)$) with nonequivalent $^1H-^{13}C$ couplings. In model II, it is assumed that the spin system consists of two different and isolated methylenes ($^1H(1)-^{13}C-^1H(1)$ and $^1H(2)-^{13}C-^1H(2)$) with identical heteronuclear interactions within each group. The two couplings, $^{13}C-^1H(1)$ and $^{13}C-^1H(2)$, were estimated from the splittings in the PDLF subspectrum. The line shapes calculated for I and II clearly demonstrate that (i) the PDLF experiment cannot distinguish between the two models, (ii) model I is consistent with all experimental data, and (iii) model II, corresponding to density modulations, is excluded on the basis of the SLF and PISEMA results.

Before closing this section, we comment on the 2D exchange experiments reported in the ^2H NMR study of RufH8O$-^2H_\alpha$,[3] where a slow exchange process was observed between the inner and the outer ^2H quadrupolar doublets. This process, with correlation times between 2 and 75 ms, was ascribed to dynamic packing fluctuations along the columns. Assuming that the two doublets instead originate from nonequivalent deuterons within the same α methylene group, possible explanations of the

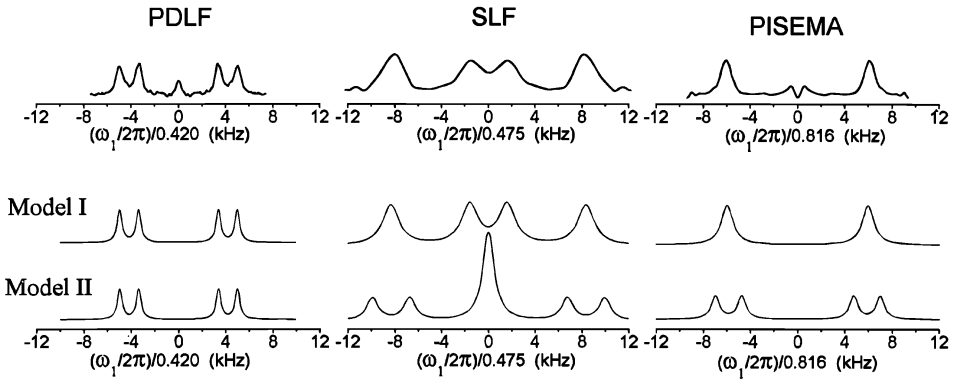

Figure 14. Experimental α_3 methylene slices obtained at 40 °C using the PDLF, SLF and PISEMA pulse sequences (top row). Simulations for models I and II (explained in the text) are shown in the middle and bottom rows, respectively. The following dipolar couplings were used in the simulations: $^1H(1)-^{13}C = 5.0$ kHz and $^1H(2)-^{13}C = 3.4$ kHz. Note that all frequency axes have been corrected by the multiple-pulse scaling factors.

exchange process include: (i) slow transitions between two chain conformations symmetrically arranged with respect to the core and (ii) ^{2}H spin diffusion.[45,46]

Summary and Conclusions

We have in this work presented a separated local field study of the solid and liquid-crystalline phases of the discotic sample RufH8O. The estimated ^{1}H−^{13}C dipolar couplings are readily interpreted in terms of molecular conformation, mobility, and orientational order. The conclusions of our investigation may be summarized as follows:

(i) The structure and dynamics differ significantly for the three nonequivalent chains in RufH8O. This holds for both the solid and columnar phases.

(ii) The segmental mobility of the $^1H_\alpha-^{13}C_\alpha$ bond vectors in the solid phase decrease in the following order: α_2, α_1, and α_3. A similar situation seems to prevail in the mesophase. Most of this side chain dynamics occur about the O−C_α bond, whereas motions about the C_{core}−O bond are highly restricted.

(iii) One of the aliphatic chains (R_3) adopts an in-plane conformation, whereas R_1 and R_2 prefer out-of-plane structures.

(iv) The α_3 methylene signal exhibits two ^{1}H−^{13}C dipolar splittings at low temperatures in the columnar phase. Similar pairs of doublets have been observed in a ^{2}H NMR study of RufH8O−$^2H_\alpha$[3] and were there interpreted in terms of dynamic packing fluctuations along the columns. We have presented an alternative explanation and showed that these two doublets most likely originate from nonequivalent protons (or deuterons) in the α_3 methylene group and not from density modulations. Of course, this result does not exclude the possibility that packing fluctuations occur in the liquid-crystalline phases of RufH8O. It only shows that it is not necessary to invoke this effect in explaining the experimental NMR data sets published to date.

Acknowledgment. We acknowledge useful discussions with Xin Zhao. This work was supported by the Swedish Research Council, the Carl Trygger Foundation, the Magn. Bergvall Foundation, and the Deutscher Akademischer Austauschdienst together with the Swedish Institute under Project No. 313-S-PPP-7/98.

References and Notes

(1) Chandrasekhar, S.; Sadashiva, B. K.; Suresh, K. A. *Pramana India* **1977**, *9*, 471−480.
(2) Dvinskikh, S.; Sandström, D.; Luz, Z.; Zimmermann, H.; Maliniak, A. **2003**, Submitted.
(3) Werth, M.; Leisen, J.; Boeffel, C.; Dong, R. Y.; Spiess, H. W. *J. Phys. II Fr.* **1993**, *3*, 53−67.
(4) Hollander, A.; Hommels, J.; Prins, K. O.; Spiess, H. W.; Werth, M. *J. Phys. II Fr.* **1996**, *6*, 1727−1741.
(5) Krishnan, K.; Balagurusamy, V. S. K. *Mol. Cryst. Liq. Cryst.* **2000**, *350*, 1−18.
(6) de Gennes, P. G. *J. Phys. Lett. (Paris)* **1983**, *44*, L657−L664.
(7) Zimmermann, H. *Liq. Cryst.* **1989**, *4*, 591−618.
(8) Metz, G.; Wu, X.; Smith, S. O. *J. Magn. Reson. Ser. A* **1994**, *110*, 219−227.
(9) Zhao, X.; Edén, M.; Levitt, M. H. *Chem. Phys. Lett.* **2001**, *342*, 353−361.
(10) Carravetta, M.; Edén, M.; Zhao, X.; Brinkmann, A.; Levitt, M. H. *Chem. Phys. Lett.* **2000**, *321*, 205−215.
(11) Brinkmann, A.; Levitt, M. H. *J. Chem. Phys.* **2001**, *115*, 357−384.
(12) Brinkmann, A.; Carravetta, M.; Zhao, X.; Edén, M.; Schmedt auf der Günne, J.; Levitt, M. H. Using symmetry to design pulse sequences in solid-state NMR. In *Perspectives on Solid State NMR in Biology*; Kiihne, S. R., De Groot, H. J. M., Eds.; Kluwer: Dordrecht, 2001; pp 3−14.
(13) Levitt, M. H. Symmetry-based pulse sequences in magic-angle spinning solid-state NMR. In *Encyclopedia of Nuclear Magnetic Resonance*; Grant, D. M., Harris, R. K., Eds.; Wiley: Chichester, U.K., 2002; pp 165−196.
(14) Bennett, A. E.; Rienstra, C. M.; Auger, M.; Lakshmi, K. V.; Griffin, R. G. *J. Chem. Phys.* **1995**, *103*, 6951−6958.
(15) Hester, R. K.; Ackerman, J. L.; Neff, B. L.; Waugh, J. S. *Phys. Rev. Lett.* **1976**, *36*, 1081−1083.
(16) Schmidt-Rohr, K.; Spiess, H. W. *Multidimensional solid-state NMR and polymers*; Academic Press: London, 1994.
(17) Nakai, T.; Terao, T. *Magn. Reson. Chem.* **1992**, *30*, 42−44.
(18) Schmidt-Rohr, K.; Nanz, D.; Emsley, L.; Pines, A. *J. Phys. Chem.* **1994**, *98*, 6668−6670.
(19) Fung, B. M.; Ermolaev, K.; Yu, Y. *J. Magn. Reson.* **1999**, *138*, 28−35.
(20) Mansfield, P. *J. Phys. C* **1971**, *4*, 1444−1447.
(21) Rhim, W. K.; Elleman, D. D.; Vaughan, R. W. *J. Chem. Phys.* **1973**, *59*, 3740−3749.
(22) Burum, D. P.; Linder, M.; Ernst, R. R. *J. Magn. Reson.* **1981**, *44*, 173−188.
(23) Mehring, M.; Waugh, J. S. *Phys. Rev. B* **1972**, *5*, 3459−3471.
(24) Bielecki, A.; Kolbert, A. C.; Levitt, M. H. *Chem. Phys. Lett.* **1989**, *155*, 341−346.
(25) Bielecki, A.; Kolbert, A. C.; De Groot, H. J. M.; Griffin, R. G.; Levitt, M. H. *Adv. Magn. Reson.* **1990**, *14*, 111−124.
(26) Palmas, P.; Tekely, P.; Canet, D. *J. Magn. Reson. Ser. A* **1993**, *104*, 26−36.
(27) Wu, C. H.; Ramamoorthy, A.; Opella, S. J. *J. Magn. Reson. Ser. A* **1994**, *109*, 270−272.
(28) Ramamoorthy, A.; Wu, C. H.; Opella, S. J. *J. Magn. Reson.* **1999**, *140*, 131−140.
(29) Fu, R.; Tian, C.; Cross, T. A. *J. Magn. Reson.* **2002**, *154*, 130−135.
(30) Hong, M.; Pines, A.; Caldarelli, S. *J. Phys. Chem.* **1996**, *100*, 14815−14822.
(31) Courtieu, J.; Bayle, J. P.; Fung, B. M. *Prog. Nucl. Magn. Reson. Spectrosc.* **1994**, *26*, 141−169.
(32) Bak, M.; Rasmussen, J. T.; Nielsen, N. C. *J. Magn. Reson.* **2000**, *147*, 296−330.
(33) Hohwy, M.; Bildsøe, H.; Jakobsen, H. J.; Nielsen, N. C. *J. Magn. Reson.* **1999**, *136*, 6−14.
(34) Zaremba, S. K. *Ann. Mater. Pure Appl.* **1966**, *4*−*73*, 293.
(35) Conroy, H. *J. Chem. Phys.* **1967**, *47*, 5307−5318.
(36) Cheng, V. B.; Suzukawa, H. H.; Wolfsberg, M. *J. Chem. Phys.* **1973**, *59*, 3992−3999.
(37) Suwelack, D.; Rothwell, W. P.; Waugh, J. S. *J. Chem. Phys.* **1980**, *73*, 2559−2569.
(38) Rothwell, W. P.; Waugh, J. S. *J. Chem. Phys.* **1981**, *74*, 2721−2732.
(39) Emsley, J. W. *Nuclear Magnetic Resonance of Liquid Crystals*; Reidel: Dordrecht, Holland, 1985.
(40) Dong, R. Y. *Nuclear Magnetic Resonance of Liquid Crystals*; Springer: New York, 1994.
(41) Luz, Z.; Goldfarb, D.; Zimmermann, H. Discotic Liquid Crystals and Their Characterization by Deuterium NMR. In *Nuclear Magnetic Resonance of Liquid Crystals*; Emsley, J. W., Eds.; Reidel: Dordrecht, Holland, 1985; pp 343−377.
(42) Ishii, Y.; Terao, T.; Hayashi, S. *J. Chem. Phys.* **1997**, *107*, 2760−2774.
(43) Poupko, R.; Luz, Z.; Spielberg, N.; Zimmermann, H. *J. Am. Chem. Soc.* **1989**, *111*, 6094−6105.
(44) Emsley, J. W. Liquid crystalline samples: structure of nonrigid molecules. In *Encyclopedia of nuclear magnetic resonance*; Grant, D. M., Harris, R. K., Eds.; Wiley: Chichester, U.K., 1996; pp 2781−2787.
(45) Suter, D.; Ernst, R. R. *Phys. Rev. B* **1985**, *32*, 5608−5627.
(46) Müller, A.; Haeberlen, U. *Chem. Phys. Lett.* **1996**, *248*, 249−254.